

## Femtosecond Pulse Propagation through a Quantum Wire Optical Waveguide Observed by Cross-Correlation Frequency-Resolved Optical Gating Spectroscopy

Noriaki TSURUMACHI<sup>1,2,\*</sup>, Naoki WATANABE<sup>3</sup>, Kazunori HIKOSAKA<sup>1,2</sup>, Xue-Lun WANG<sup>1,2</sup>, Kazuhiro KOMORI<sup>1,2</sup>, Toshiaki HATTORI<sup>3</sup> and Mutsuo OGURA<sup>1,2</sup>

<sup>1</sup>National Institute of Advanced Industrial Science and Technology (AIST), 1-1-1 Umezono, Tsukuba, Ibaraki 305-8568, Japan

<sup>2</sup>CREST-Japan Science and Technology Corporation (JST), 4-1-8 Honcho, Kawaguchi, Saitama 332-0012, Japan

<sup>3</sup>Institute of Applied Physics, University of Tsukuba, 1-1-1 Tennodai, Tsukuba, Ibaraki, Japan

(Received September 22, 2003; accepted December 2, 2003; published April 27, 2004)

Femtosecond optical pulse propagation in a quantum wire (QWR) waveguide was investigated by two-color sum-frequency cross-correlation frequency-resolved optical gating (XFROG) spectroscopy. The polarization anisotropy of the crescent-shaped GaAs QWR was observed in terms of absorption and refractive index dispersion by XFROG spectroscopy.

[DOI: 10.1143/JJAP.43.2002]

KEYWORDS: quantum wire, waveguide, pulse propagation, XFROG, anisotropy

### 1. Introduction

An optical waveguide containing quantum nano structures is an important component of ultrafast photonic devices such as laser diodes, semiconductor optical amplifiers, and photonic switches. The analysis of ultrashort optical pulse propagation properties is essential for the optimum design of these devices. However, the distortion of optical ultrashort pulses transmitted through them is very complicated, because both the amplitude and the phase are changed by numerous linear optical factors such as refractive index dispersion, absorption and gain, and nonlinear optical effects such as two-photon absorption and self-phase modulation.<sup>1,2)</sup> Therefore, transmission properties of the optical waveguide in both time and frequency domains should be fully characterized in advance for the design of future photonic devices.

Recently, frequency-resolved optical gating (FROG) has frequently been applied to full characterization of ultrashort optical pulses, since it yields information on both the amplitude and phase of a pulse field.<sup>3)</sup> Although second-harmonic generation FROG (SHG-FROG) is one of the most widely used methods of ultrashort pulse characterization,<sup>4)</sup> it often fails to retrieve a weak pulse. Cross-correlation FROG (XFROG) is more suitable for weak pulse characterization than SHG-FROG because this technique is based on the sum-frequency signal between a weak test pulse and a strong gated pulse.<sup>5,6)</sup> Since the amplitude and the phase of the pulse in the time domain can easily be transformed to the amplitude and the phase information in the frequency domain, this XFROG technique can be applied to the measurement of the complex transmission coefficient of a sample in a linear regime. Not only the complex transmission coefficient in the frequency domain, but also the deformation of the ultrashort pulses in the time domain can be observed directly at the same time in both linear and nonlinear regions by XFROG spectroscopy.<sup>7–10)</sup> In this study, the transmission properties including the polarization anisotropy of the quantum wire (QWR) waveguide are investigated by the XFROG spectroscopy.

### 2. Experimental Procedure

Both the amplitude and phase information of a light field can be obtained by the XFROG method. XFROG spectroscopy is based on the intensity cross-correlation measurement. The electric field of the cross-correlation signal  $E_{\text{cross}}$  has the form for sum-frequency generation of

$$E_{\text{cross}}(t, \tau) = E_{\text{gate}}(t)E_{\text{test}}(t - \tau), \quad (1)$$

where  $E_{\text{gate}}$  and  $E_{\text{test}}$  are the electric fields of the gated and test pulses, respectively. The spectrum of the cross-correlation recorded as a function of delay  $\tau$  between the test and gated pulses yields the XFROG trace as

$$I_{\text{XFROG}}(\omega, \tau) = \left| \int_{-\infty}^{+\infty} E_{\text{cross}}(t, \tau) \exp(i\omega t) dt \right|^2. \quad (2)$$

The XFROG algorithm based on iterative Fourier transformation with generalized projection is performed to retrieve an unknown test pulse.<sup>5)</sup> This algorithm requires input data of both the experimentally obtained XFROG trace  $I_{\text{XFROG}}(\omega, t)$  and the electric field of the gated pulse  $E_{\text{gate}}(t)$ , which is previously well characterized by another method, for instance, SHG-FROG. Starting with an initial guess of the test pulse, the iterative Fourier transform algorithm generates a better guess, which approaches the correct complex electric field. The complex transmission properties of a sample can be derived from the amplitude and phase information of both the input and output light fields. Thus, the XFROG method can be applied as a spectroscopic tool for the characterization of the optical properties of a sample such as a waveguide structure.

In this study, we employed XFROG spectroscopy to obtain the complex transmission properties of a semiconductor optical waveguide with GaAs/AlGaAs QWRs. Figure 1 shows a cross-sectional high-resolution scanning electron microscopy (SEM) image of the QWR waveguide sample. The QWR sample was an optical waveguide containing 7-period crescent-shaped GaAs/Al<sub>0.36</sub>Ga<sub>0.64</sub>As QWRs fabricated by flow rate modulation epitaxy.<sup>11–13)</sup> The cladding layer was Al<sub>0.63</sub>Ga<sub>0.37</sub>As. The (001) flat and (111)A sidewall regions were removed selectively by wet chemical etching, which is effective in suppressing the PL from parasitic QWs of the sample.<sup>12)</sup> The PL from the QWR is located at 795 nm. Here, the length of the waveguide was

\*Correspondence address: Faculty of Engineering, Kagawa University, 2217-20 Hayashi-cho, Takamatsu, Kagawa, Japan. E-mail address: tsuru@eng.kagawa-u.ac.jp

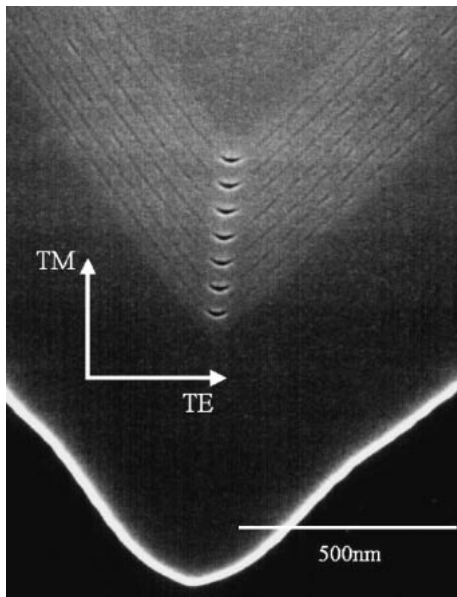


Fig. 1. Cross-sectional SEM image of the QWR waveguide structure.

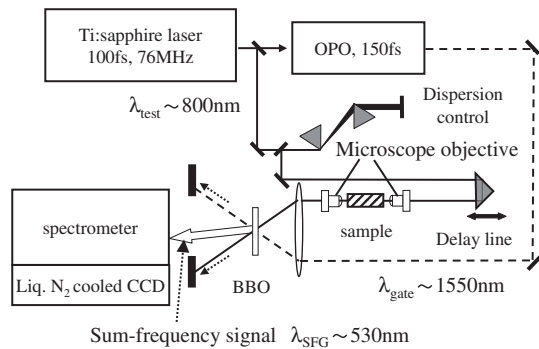


Fig. 2. Schematic of the experimental setup for XFROG spectroscopy.

1000  $\mu\text{m}$ . The horizontal and vertical directions correspond to the TE-like and TM-like polarization modes of the waveguide, respectively, as shown by arrows in Fig. 1.

Figure 2 shows a schematic of the experimental setup used in this measurement. The laser system used was based on a mode-locked Ti:sapphire laser and an optical parametric oscillator (OPO). The output from the Ti:sapphire laser, whose wavelength and pulse duration were approximately 800 nm and approximately 100 fs, respectively, was focused onto the waveguide facet by a microscope objective with a magnitude of 20 after chirp compensation using a prism pair. The spot diameter of the incident laser at the waveguide facet was about 5  $\mu\text{m}$ . A part of the Ti:sapphire laser output was used to pump the OPO. The transmitted and gated pulses from the OPO, whose wavelength and pulse duration were around 1550 nm and about 150 fs, were overlapped on a 0.5-mm-thin  $\beta\text{-BaB}_2\text{O}_4$  (BBO) crystal and sum-frequency light was generated. The sum-frequency light spectra were recorded with a liquid-N<sub>2</sub>-cooled CCD camera as a function of the delay between the transmitted and gated pulses. We refer to them as XFROG traces. By retrieving the phase from an experimentally obtained XFROG trace,<sup>5,6)</sup> we obtained both the amplitude and phase of the pulse.

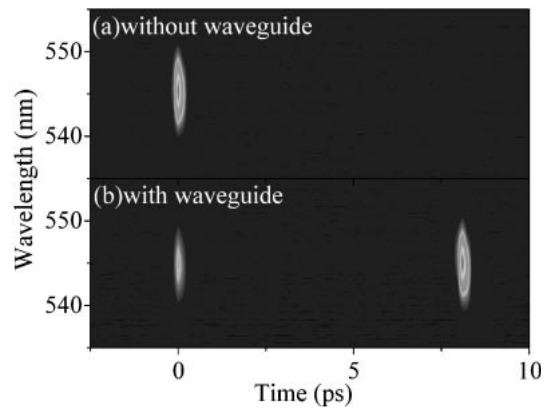


Fig. 3. Typical results of the XFROG measurement for (a) without a sample and (b) with a sample.

The XFROG method is a powerful tool for the characterization of the pulse particularly when the pulse intensity is weak. If the wavelengths of the test and gated pulses are the same, the wavelength of the second-harmonic light of each pulse and that of the cross-correlation signal are the same. Since the scattered second harmonics of a strong gated pulse may be a strong background if the cross-correlation signal is weak, background-free measurements are desirable. The combination of the Ti:sapphire laser and the OPO (two-color configuration) provides a background-free measurement. Since the wavelengths of the sum-frequency signal and the SHG signal from each of the pulses are different, the sum-frequency signal can be easily resolved by a spectrometer.<sup>14)</sup>

The waveguide sample was fixed on the cold finger of a high-stability transmission-type helium cryostat (Axess Tech) for the low-temperature experiment. The drift of the sample position with respect to the support of the cryostat in all dimensions was less than 1 micron for at least over 3 h. CCD cameras were used in order to visualize the waveguide facet on both input and output sides.

Figure 3 shows the typical result of the XFROG measurement for (a) without a sample and (b) with a sample. The sum-frequency cross-correlation signal is generated at  $t = 0$  in Fig. 3(a); on the other hand in Fig. 3(b), the strong correlation signal appears at around  $t = 8.1$  ps and a weak signal still remains at  $t = 0$ . This strong signal is attributed to the cross-correlation between the waveguide transmitted light and the gated light, and the weak signal at  $t = 0$  is due to the stray light out of the waveguide. Here, the sample was a GRIN-SCH optical waveguide containing GaAs/AlGaAs QWs and the input light wavelength was in the off resonant region. The length of the waveguide was 700  $\mu\text{m}$ . In the case of the conventional cw transmission spectroscopy of waveguide structures, it is necessary to separate the light transmitted through the waveguide spatially from the stray light, which does not enter the waveguide core region due to the loose focus or misalignment, so that the measurement of the transmission spectrum was comparatively difficult. On the other hand, in this XFROG case, these two different components are easily separated by time-resolved measurement since the arrival of the transmitted light through the optical waveguide to the BBO crystal is delayed. By phase retrieval of the XFROG trace of the transmitted light through

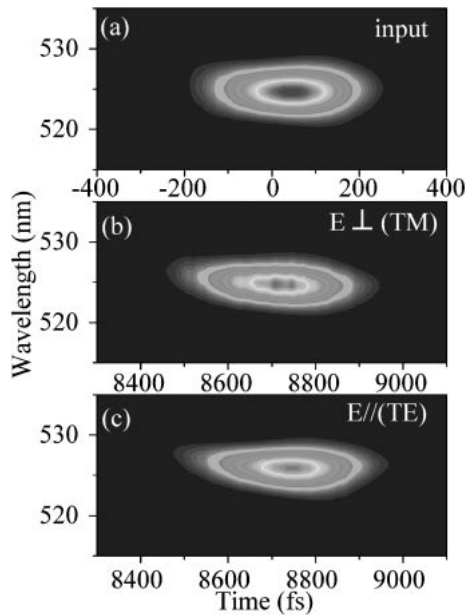


Fig. 4. Experimentally obtained XFROG traces for (a) the input pulse, (b) the TM polarization output, and (c) the TE polarization output in the resonant experiment of the QWR waveguide.

the waveguide (in this case, around  $t = 8.1$  ps), the amplitude and the phase information of the transmitted light can be obtained.

### 3. Results and Discussion

The results of the XFROG experiment for the case of the resonant condition in the QWR waveguide are described. Figure 4 shows the experimentally obtained XFROG traces for (a) the input pulse, (b) the output pulse from the waveguide when the light was TM-like-polarized (vertical) and (c) the output when the light was TE-like-polarized (horizontal). We observed the polarization anisotropy of the QWR waveguide by the phase retrieval from these traces. Figure 5 shows the retrieved normalized transmitted intensity and group delay dispersion in the frequency domain. The peak of the output light spectrum of the TE polarization is red shifted compared with that of the TM polarization due to the occurrence of absorption on the higher energy side. The group delay dispersion of the TM polarization is almost straight. However, that of the TE polarization bends at 1.57 eV, which reflects an anomalous dispersion related to the absorption. These differences between the TE and TM polarizations are attributed to the absorption anisotropy of the QWRs. The polarization anisotropy has been shown to depend strongly on the cross-sectional QWR shape. Martinet *et al.* discussed the absorption anisotropy in a crescent-shaped QWR waveguide between TE and TM polarizations.<sup>15)</sup> They found a new genuine QWR transition in TM polarization  $e_1h_2$ , which arises from both valence band mixing at  $k = 0$  and symmetry breaking at the heterostructural level, despite the mirror symmetry. In the TM polarization, the  $e_1h_1$  transition has no visible feature and the  $e_1h_2$  transition is the lowest one which is located on the higher energy side from the  $e_1h_1$  transition. Our results also suggest that the absorption edge in the TM polarization is located at a higher energy compared with that in the TE

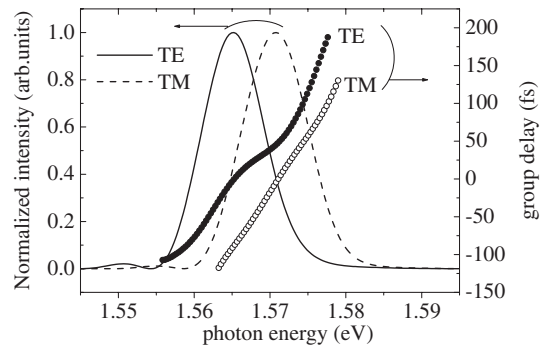


Fig. 5. Intensity and the group delay dispersion in the frequency domain retrieved from the XFROG trace. Solid line is the intensity of the TE polarization and dashed line is that of the TM polarization. Dotted line is that of the input. Closed circle is group delay of the TE polarization and open circle is that of the TM polarization.

polarization.

Although the experimentally obtained XFROG traces were not completely the same as shown in Fig. 4, for example the position of the top of contour, they are quite similar and it is difficult to mutually distinguish them clearly for both polarizations. This is because the active volume of QWRs is quite small compared with the case of QWs in general, so that the influence of the absorption during the propagation is also comparatively small. Therefore, it is necessary to perform the phase retrieval of XFROG traces in order to discuss the anisotropy of absorption. As mentioned above, we could observe the polarization anisotropy of the QWR when the light propagates along the QWR. In order to evaluate the detailed optical properties of QWR such as the detailed absorption spectrum profile, it is necessary to optimize the absorption coefficient, waveguide length, waveguide modes and coupling constant of the waveguide. Here, we emphasize that the anisotropy of dispersion in a QWR optical device could be clearly observed by this XFROG spectroscopy even for a comparatively small signature of QWR absorption.

### 4. Conclusions

We investigated the femtosecond pulse propagation effects in a semiconductor QWR waveguide by XFROG spectroscopy. In the QWR waveguide, the polarization anisotropy of the QWR could be observed by XFROG spectroscopy despite the small absorption. XFROG spectroscopy was shown to be a very simple and valuable technique for the characterization of waveguide-semiconductor photonic devices, since the transmission properties such as pulse shape, chirping, absorption and dispersion spectra can be easily obtained at the same time using this technique.

- 1) F. Romstad, P. Borri, W. Langbein, J. Mørk and J. M. Hvam: IEEE Photon. Technol. Lett. **12** (2000) 1674.
- 2) N. Bélanger, A. Villeneuve and J. S. Aitchison: J. Opt. Soc. Am. B **14** (1997) 3003.
- 3) R. Trebino, K. W. Delong, D. N. Fittinghoff, J. N. Sweetser, M. A. Krumbügel, B. A. Richman and D. J. Kane: Rev. Sci. Instrum. **68** (1997) 3277.
- 4) A. Baltuška, M. S. Pshenichnikov and D. Wiersma: Opt. Lett. **23**

- (1998) 1474.
- 5) S. Linden, H. Giessen and J. Kuhl: *Phys. Status Solidi B* **206** (1998) 119.
  - 6) S. Linden, J. Kuhl and H. Giessen: *Opt. Lett.* **24** (1999) 569.
  - 7) Y. Mitsumori, R. Kawahara, T. Kuroda and F. Minami: *J. Lumin.* **94–95** (2001) 645.
  - 8) A. Yabushita, T. Fuji and T. Kobayashi: *Opt. Commun.* **198** (2001) 227.
  - 9) N. Nishizawa and T. Goto: *Opt. Exp.* **8** (2001) 328.
  - 10) N. Tsurumachi, K. Hikosaka, X.-L. Wang, M. Ogura, N. Watanabe and T. Hattori: *J. Appl. Phys.* **94** (2003) 2616.
  - 11) X. L. Wang, M. Ogura and H. Matsuhata: *Appl. Phys. Lett.* **66** (1995) 1506.
  - 12) X. L. Wang, M. Ogura and H. Matsuhata: *Appl. Phys. Lett.* **67** (1995) 804.
  - 13) X. Q. Liu, X. L. Wang and M. Ogura: *Appl. Phys. Lett.* **79** (2001) 1622.
  - 14) S. Haacke, R. A. Taylor, I. Bar-Joseph, M. J. S. P. Brasil, M. Hartig and B. Deveaud: *J. Opt. Soc. Am. B* **15** (1998) 1410.
  - 15) E. Martinet, M.-A. Dupertuis, L. Sirigu, D. Y. Oberli, A. Rudra, K. Leifer and E. Kapon: *Phys. Status Solidi A* **178** (2000) 233.